International Journal of Pharmacology

Int. J. Pharmacol. **2025**; 21(5): 44188
https://doi.org/10.31083/IJP44188

Research Article

Antitumor and Immunomodulatory Effects of *Periplaneta americana* Extract Combined With 5-Fluorouracil on Hepatocarcinoma Mice

Ran Gao[1,†], Rui Yuan[1,†], Guangjun Wu[1], Yan Wang[1], Meixian Guo[1,*], Xiaobo Liu[1,*]

[1]Yunnan Provincial Key Laboratory of Entomological Biopharmaceutical R&D, College of Pharmacy, Dali University, 671000 Dali, Yunnan, China
*Correspondence: yndllyo@126.com (Meixian Guo); yndlxb@126.com (Xiaobo Liu)
[†]These authors contributed equally.

Academic Editor: Mehmet Ozaslan
Published: 22 September 2025

Abstract

Background and Objective: *Periplaneta americana* is an important traditional medicine in China. Moreover, *Periplaneta americana* is effective in treating multiple tumor types. Thus, this study aimed to investigate the combined effects of *Periplaneta americana* extract CII-3 (an active component from *Periplaneta americana*) and 5-fluorouracil (5-FU) on liver cancer in mice, focusing on anti-tumor and immunomodulatory properties. **Materials and Methods**: Mice were divided into five groups: normal, model, CII-3, 5-FU and 5-FU+CII-3. Continuous treatment for 14 days included monitoring tumor volume and weight, calculating spleen and thymus indices, and observing tumor tissue morphology. Immunological assays evaluated natural killer (NK) cell cytotoxicity, T/B lymphocyte proliferation, and the proportions of CD3+, CD4+, and CD8+ cells. ELISA was employed to assess serum levels of IgA, IgM, IgG, and interleukin-8 (IL-8). The reverse transcription quantitative polymerase chain reaction (RT-qPCR) and Western blot assay were utilized to analyze the mRNA and protein expressions, respectively, of toll-like receptor 4 (TLR4), nuclear factor-kappa B (NF-κB), tumor necrosis factor receptor-associated factor 6 (TRAF6), myeloid differentiation primary response protein 88 (MyD88) and tumor necrosis factor-α (TNF-α) in tumors. **Results**: Compared to the 5-FU group, the 5-FU+CII-3 group showed reduced tumor mass and increased spleen and thymus indices. Tumor tissue in the treatment groups exhibited a loose structure, characterized by nuclear fragmentation and the presence of lipid vacuoles. The 5-FU+CII-3 group exhibited enhanced NK cell cytotoxicity, T/B lymphocyte proliferation, CD3+ proportion, CD4+/CD8+ ratio and serum levels of IgA, IgM, and IgG, alongside a reduction in IL-8 content. The levels of TLR4, NF-κB, MyD88, and TNF-α mRNA and protein expressions were downregulated, while *TRAF6* mRNA expression was also notably decreased in the tumor tissue. **Conclusion**: The CII-3 and 5-FU combined treatment synergistically exerts anti-tumor and immunomodulatory effects, potentially mediated through the regulation of TLR4, NF-κB, TRAF6, MyD88, and TNF-α.

Keywords: *Periplaneta americana* extract; 5-fluorouracil; hepatocellular carcinoma; synergism; immunoregulation

1. Introduction

Hepatocellular Carcinoma (HCC) ranks as the third leading cause of cancer-related mortality, with a 5-year survival rate of $\leq$5% in advanced stages, posing a severe threat to human life and health [1]. The HCC, one of the most critical primary liver cancers, is a major contributor to cancer-related deaths, exhibiting a male-to-female incidence ratio ranging from 2:1 to 8:1 [2,3]. The complex etiology of HCC remains unclear and its occurrence is closely associated with factors such as viral infections, fatty liver disease, diabetes, alcoholic liver disease, non-alcoholic fatty liver disease and consumption of aflatoxin-contaminated food [4]. Despite advancements in the diagnosis and treatment of HCC in recent years, the insidious onset, difficulty in early detection and the diagnosis of over 70% of patients at an advanced stage pose significant challenges [5].

The expression of Toll-Like Receptor 4 (TLR4) has been linked to the progression, invasion, metastasis and adverse prognosis of HCC [6,7]. The TLR4 is expressed on the surface of tumor cells in many different tissues and is associated with the establishment and maintenance of tumor immune microenvironment. The activation of TLR4 signaling pathway in tumor tissue can cause the increase of immunosuppressive factors, promote cancer cell proliferation and immune escape and lead to the growth and metastasis of cancer cells [8,9]. The TLR4 can activate downstream signals through myeloid differentiation primary response protein 88 (MyD88), triggering the activation of important proteins such as nuclear factor-kappa B (NF-κB). It further promotes the synthesis and release of downstream cytokines such as tumor necrosis factor-α (TNF-α), interleukin (IL)-2, IL-8 and participates in the occurrence and development of liver cancer and the production of inflammation [10]. Thus, the TLR4/MyD88/NF-κB cascade reaction is considered to be associated with the induction of liver inflammation and the progression of HCC.

Chemotherapy remains one of the most effective treatment options for advanced-stage HCC and 5-Fluorouracil (5-FU) is a commonly used chemotherapy drug in clinical practice [11]. The 5-FU intervenes in the biological behavior of HCC cells through multiple pharmacological mechanisms. Firstly, it is converted into active metabo-

lites that disrupt the synthesis of purines and pyrimidines, causing abnormal DNA and RNA synthesis, thereby hindering the normal proliferation of cancer cells. Secondly, the binding of active metabolites to DNA induces DNA strand damage, triggering apoptosis in cancer cells [12]. Additionally, the 5-FU metabolic product, 5-Fluoro-2′-Deoxyuridine Monophosphate (FdUMP), inhibits thymidylate synthase, affecting DNA synthesis and repair [13]. However, despite the significant inhibitory effects of 5-FU in HCC treatment, its usage is associated with a range of potential toxic side effects. The 5-FU can lead to bone marrow suppression, immune suppression, gastrointestinal toxicity, immune system suppression, skin reactions and neurotoxicity [9,14]. Moreover, with prolonged treatment courses, issues such as decreased drug sensitivity and drug resistance leading to poor efficacy may arise [15].

Numerous studies have indicated that the combination of traditional Chinese medicine (TCM) and chemotherapy can synergistically enhance therapeutic effects, alleviate chemotherapy side effects, improve the quality of life for patients and prolong survival time [16,17]. The TCM can suppress the occurrence of HCC by inhibiting the expression of MyD88, TRAF6, NF-κB and TNF-α [18,19]. The TCM can also modulate immune responses, inhibit the proliferation and metastasis of tumor cells [20] and rapidly identify and eliminate tumor cells, reshape the tumor microenvironment and inhibit tumor growth. The TCM achieves this by activating the functions of immune cells [21,22]. The *Periplaneta americana* has a long history of medicinal use and exhibits pharmacological activities such as anti-tumor and immune modulation [23]. The CII-3, an active component extracted from *Periplaneta americana*, has been identified as possessing anti-tumor efficacy and research suggests that its anti-tumor effects may be related to its immunomodulatory function [24]. A total of 571 peptide sequences were discovered and 329 precursor proteins were identified in CII-3 [25]. The CII-3 can enhance the immune organ indices in tumor-bearing mice, increase the number of peripheral blood immune cells, regulate the body's immune function and inhibit tumor growth [26].

Given this background, this study explored the synergistic effects and immunomodulatory actions of the *Periplaneta americana* extract CII-3 in combination with 5-fluorouracil in the treatment of HCC. This study aimed to investigate the changes in the TLR4/MyD88/NF-κB signaling pathway within the tumor and elucidate its underlying mechanisms.

2. Materials and Methods

2.1 Study Area

The current work was performed at the Yunnan Provincial Key Laboratory of Entomological Biopharmaceutical R&D, Dali University, China from October, 2023 to January, 2024.

The CII-3 extract (Batch: 20200814) was generously provided by Associate Professor Zhengchun He from the School of Pharmacy at Dali University. The extraction process involved ethanol extraction and concentration of dried *Periplaneta americana* bodies to obtain a crude extract. Further purification was achieved through chromatography using large-pore adsorption resin, alcohol elution and vacuum concentration, resulting in a refined substance primarily composed of small peptides with anti-tumor activity [27].

2.2 Animals and Cell Lines

The SPF-grade KM mice (n = 30, both genders, body weight: 18–22 g) were supplied by Hunan Slake Jingda Experimental Animal Co. Ltd. The H22 hepatocellular carcinoma cell line and Yac-1 cell line were generously provided by the Pharmacology Laboratory at Dali University. All cell lines were validated by STR profiling and tested negative for mycoplasma.

2.3 Reagents

The RPMI-1640 medium (ThermoFisher Biochemical Products, Beijing, China, Co., Ltd., No: C11875500BT); Fetal bovine serum (Hangzhou Sijiqing Biotechnology Materials, Hangzhou, China, Co. Ltd., No.: 11012-8611); Lipopolysaccharide (Beijing Solabe Biotechnology, Beijing, China, Co., Ltd., No.: L8880); Concanavalin A (Sigma, St. Louis, MO, USA, Lot: SLBL3798V); FITC Hamster Anti-Mouse CD3e, APC Rat Anti-Mouse CD4, PerCP-Cy5.5 Rat Anti-Mouse CD8a (BD, San Diego, CA, USA, No.: 553061, 553051, 551162); Total RNA extraction kit, cDNA first-strand synthesis kit, SuperReal fluorescent quantitative pre-mixed kit (Tiangen Biotech, Beijing, China, Co. Ltd., No.: DP419, KR116, FP205); Mouse IgA Elisa KIT, Mouse IgM Elisa KIT, Mouse IgG Elisa KIT (Shanghai Enzyme-linked Biotechnology, Shanghai, China, Co. Ltd., No.: ml037606, ml063597, ml037601); TLR4 Monoclonal antibody, MYD88 Monoclonal antibody, TNF-α Monoclonal antibody, Beta Actin Polyclonal antibody, HRP-Goat Anti-Rabbit Recombinant Secondary Antibody (H+L) (1:2000, Wuhan Sanying Biotechnology, Wuhan, China, Co. Ltd., No.: 66350-1, 67969-1, 60291-1, 20536-1, SA00001-2); Rabbit Anti p-NF-κB P65 (1:1000, Beijing Bobo Sen Biotechnology, Beijing, China, Co. Ltd., No.: bs-0982R); Rabbit TRAF6 Antibody (1:500, Wuhan Huamei Bioengineering, Wuhan, China, No.: PA004325).

2.4 Instruments

Instruments comprised an inverted microscope (CKX41SF, Olympus, Windsor, Hachioji-shi, Tokyo Metropolis, Japan), a microplate reader (255939, Bio-Teck, Winooski, VT, USA), a CO_2 incubator (5510E, NUAIRE, Plymouth, MN, USA), a flow cytometer (FACSCantoII, BD, Franklin Lakes, NJ, USA), a protein electrophoresis apparatus (1658004, Bio-Rad, Hercules,

CA, USA), a gel chemiluminescence imaging system (GelView6000Pro, Bo Lu Teng, Guangzhou, China) and a real-time fluorescence quantitative PCR analysis instrument (2720, Applied Biosystems, Carlsbad, CA, USA).

2.5 Methods

2.5.1 Establishment of the Mouse Hepatocellular Carcinoma Xenograft Model

The H22 mouse hepatocellular carcinoma cells were resuscitated, adjusted to a density of 1×10^7 cells/mL with PBS and intraperitoneally inoculated into mice at 0.2 mL per mouse. After 7 days of cultivation, ascites were collected and H22 cell suspension (1×10^7 cells/mL, 0.2 mL) was subcutaneously injected into the right forelimb axillary region to establish the hepatocellular carcinoma H22 xenograft model.

All the experiments were performed based on the approved animal protocols and guidelines established by the Medicine Ethics Review Committee for Animal Experiments of Dali University under the approval (number: 2023P2260).

2.5.2 Grouping and Drug Administration

Apart from the normal group, tumor-bearing mice were randomly divided into the model group, CII-3 125 mg/kg group, 5-Fluorouracil (5-FU) 45 mg/kg group and 5-FU 45 mg/kg+CII-3 125 mg/kg group. The blank and model groups received intragastric saline and intraperitoneal injection of 5-FU, while the CII-3 group received intragastric administration of 125 mg/kg CII-3 once a day. The combination group received both 125 mg/kg CII-3 orally and intraperitoneal injection of 45 mg/kg 5-FU every 2 days.

2.5.3 Measurement of Tumor Volume, Weight, Spleen Weight and Thymus Weight

Tumor dimensions were measured on days 6, 8, 10, 12 and 14 after administration. Tumor volume was calculated using the formula:

$$\text{Volume} = (\text{Length} \times \text{Width}^2) \times 0.5$$

Mice were euthanized by cervical dislocation 24 hours after the final administration, in accordance with institutional ethical guidelines. The weights of tumors, spleens, and thymuses were recorded. Tumor inhibition rate, spleen index, and thymus index were subsequently calculated.

2.5.4 Observation of Tumor Tissue Pathological Morphology by H&E Staining

Tumors were harvested, washed in physiological saline, fixed in 10% paraformaldehyde, processed through dehydration, paraffin embedding, sectioning, H&E staining and neutral gum sealing and observed under an optical microscope.

Table 1. qPCR primer sequences.

Genes	Sequence (5′-3′)
TLR4	
Forward	ATGGCATGGCTTACACCACC
Reverse	GAGGCCAATTTTGTCTCCACA
NF-κB	
Forward	ATGGCAGACGATGATCCCTAC
Reverse	CGGAATCGAAATCCCCTCTGTT
TRAF6	
Forward	TCATTATGATCTGGACTGCCCAAC
Reverse	TTATGAACAGCCTGGGCCAAC
MYD88	
Forward	TACAGGTGGCCAGAGTGGAA
Reverse	GCAGTAGCAGATAAAGGCATCGAA
TNF-α	
Forward	CAGGCGGTGCCTATGTCTCA
Reverse	GGCTACAGGCTTGTCACTCGAA
β-actin	
Forward	GGCTGTATTCCCCTCCATCG
Reverse	CCAGTTGGTAACAATGCCATGT

qPCR, Quantitative Polymerase Chain Reaction; *TLR4*, Toll-Like Receptor 4; *NF-κB*, Nuclear Factor-kappa B; *TRAF6*, Tumor Necrosis Factor Receptor-Associated Factor 6; *MYD88*, Myeloid Differentiation Primary Response Protein 88; *TNF-α*, Tumor Necrosis Factor-α.

2.5.5 Measurement of NK Cell Cytotoxicity and T/B Lymphocyte Proliferation Ability in Mouse Spleen

Spleens were obtained and cell suspensions were prepared by gently grinding through a cell strainer. The cell concentration was adjusted to 5×10^6 cells/mL and cells were seeded into a 96-well plate for stimulation. The MTT assay was performed after 48 hrs of incubation to determine the stimulation index. The Yac-1 cells in logarithmic growth phase were used to assess NK cell cytotoxicity. The cell concentration was adjusted to 1×10^5 cells/mL and 100 µL was added to the target cell group. The effector cell group and effector cell+target cell group were set up with 100 µL complete culture medium and 100 µL Yac-1 cells, respectively. After 48 hrs of incubation, the MTT assay was performed to calculate NK cell cytotoxicity.

2.5.6 Flow Cytometry to Detect the Proportion of CD3+, CD4+ and CD8+ Cells in Mouse Spleen

Spleen cell suspensions were prepared and the cell concentration was adjusted to 5×10^6 cells/mL. The FITC Hamster Anti-Mouse CD3e, APC Rat Anti-Mouse CD4 and PerCP-Cy5.5 Rat Anti-Mouse CD8a were used for staining. Flow cytometry was used to detect the proportions of CD3+, CD4+ and CD8+ cells in mouse spleen.

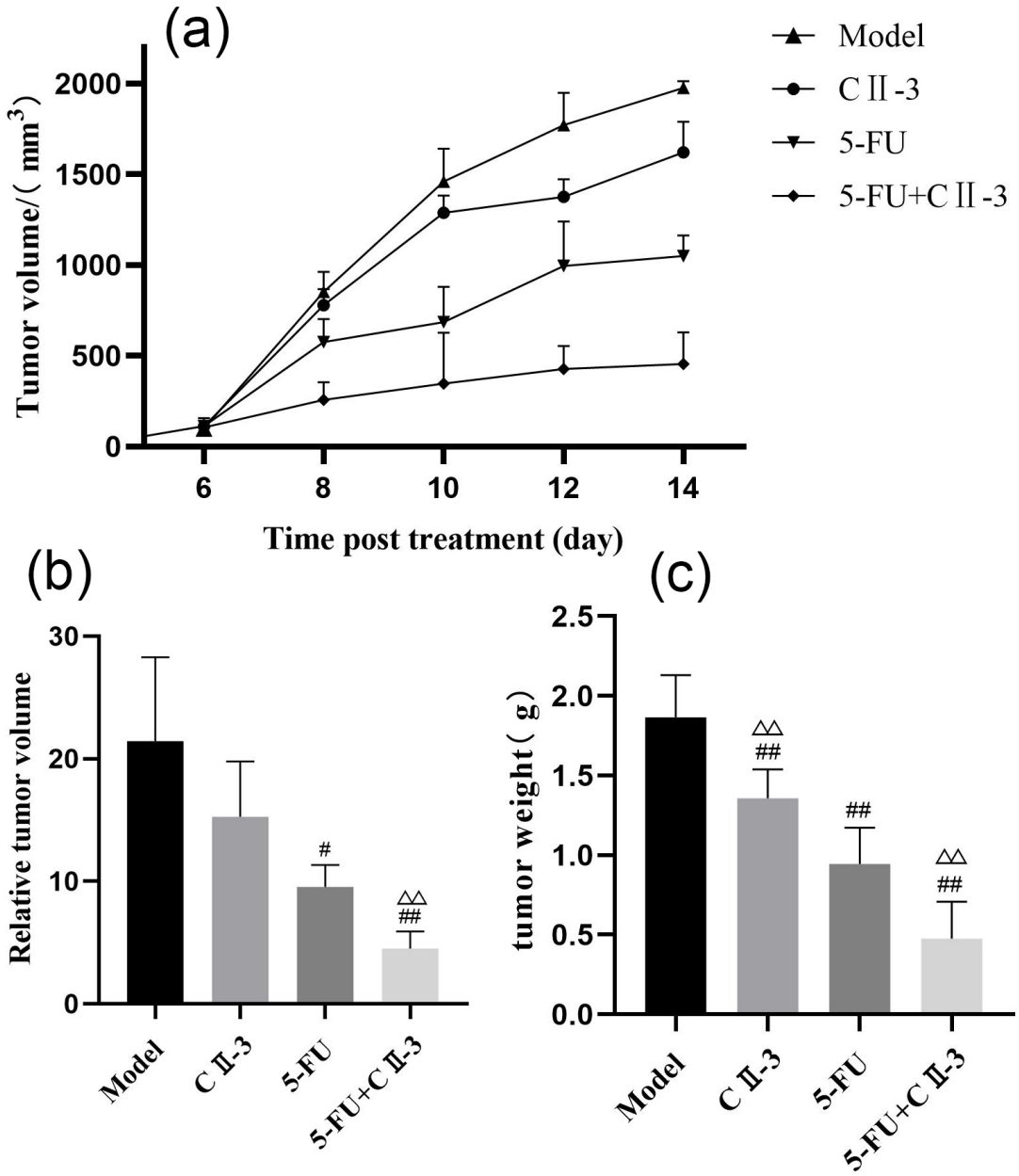

Fig. 1. Changes in weight and volume of mice tumour tissue under different exposure conditions. (a) Changes in tumor volume over time, (b) Relative tumor volume and (c) Weight of tumor tissue after 14 days . Relative tumor volumes were standardized with the tumor volume at day 6 as the baseline. n = 6. #$p < 0.05$, ##$p < 0.01$: Compared with the model group; $\Delta\Delta p < 0.01$: Compared with the 5-FU group. 5-FU, 5-fluorouracil.

2.5.7 ELISA Assay to Determine IgA, IgM, IgG and IL-8 Levels in Mouse Serum

Mouse eyeballs were removed, blood was collected to prepare serum and ELISA assays were performed to determine the levels of IgA, IgM, IgG and IL-8 according to the instructions of the respective ELISA assay kits.

2.5.8 Real-Time Fluorescence Quantitative Polymerase Chain Reaction (qPCR) to Detect the Expression of TLR4, NF-κB, TRAF6, MYD88 and TNF-α mRNA in Mouse Tumors

Total RNA was extracted from tumors using a total RNA extraction kit. Reverse transcription was performed using a cDNA synthesis kit and quantitative PCR was carried out using the SuperReal fluorescence quantitative kit. The $2^{-\Delta\Delta Ct}$ method was used to calculate the relative expression of mRNA. The qPCR primer sequences were shown in Table 1.

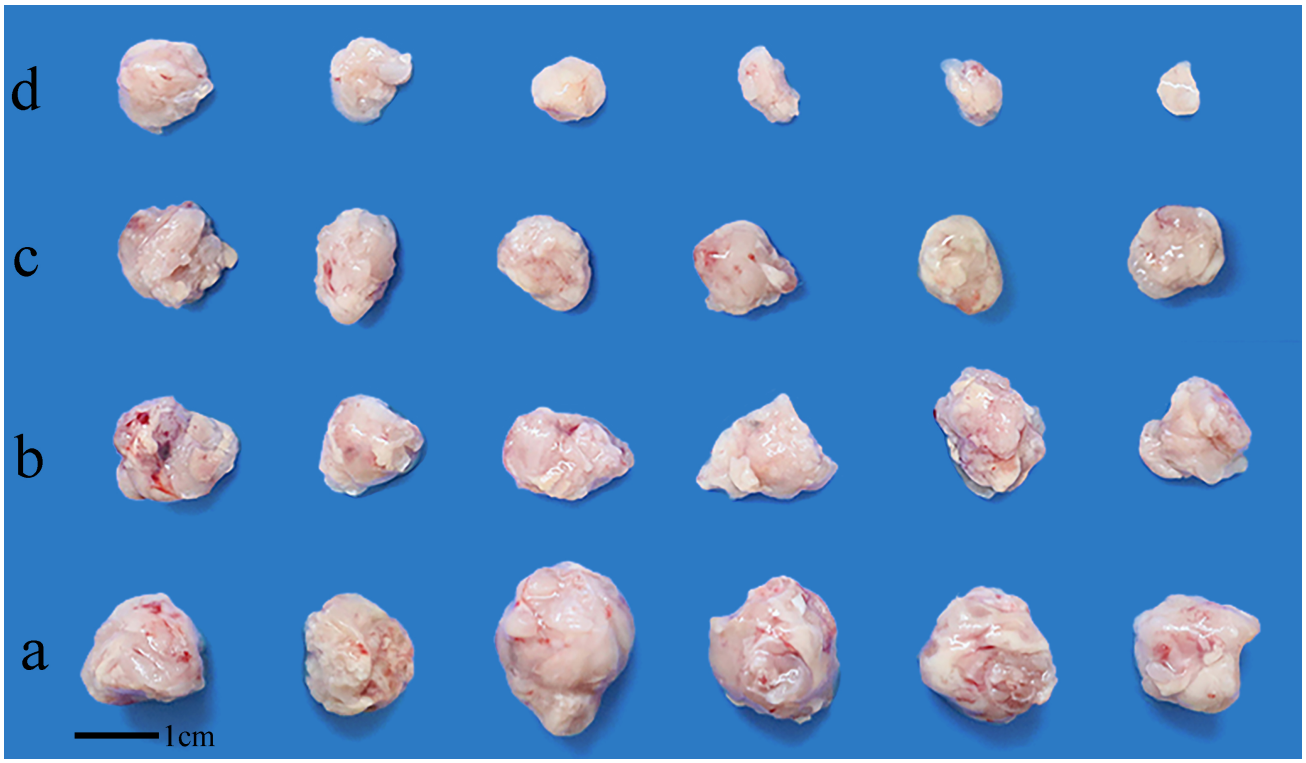

Fig. 2. Tumor tissue of mice after 14 days of different exposure conditions. (a) Model group, (b) CII-3 group, (c) 5-FU group and (d) 5-FU+CII-3 group. Scale bar = 1 cm. n = 6.

2.5.9 Western Blot to Detect the Expression of TLR4, NF-κB, TRAF6, MYD88 and TNF-α Proteins in Mouse Tumors

Tumor tissues were homogenized and total protein was extracted using RIPA lysis buffer. Protein concentration was determined using the BCA protein assay. The SDS-PAGE gel electrophoresis, PVDF membrane transfer, milk blocking, overnight incubation with primary antibodies, secondary antibody incubation, chemiluminescence imaging and grayscale value analysis using ImageJ software 1.54 (NIH, Bethesda, MD, USA). were performed. The β-actin was used as an internal reference.

2.6 Statistical Methods

The SPSS 27.0 (IBM-SPSS Statistics, Chicago, IL, USA) was used for data analysis. Measurement data were expressed as Mean $\pm$ Standard Deviation ($\bar{x} \pm s$). Homogeneity of variance test and one-way analysis of variance were used for intergroup comparison, with $p < 0.05$ and $p < 0.01$ indicating statistical significance.

3. Results

3.1 Impact of CII-3 on Tumor Volume, Tumor Weight and Tumor Inhibition Rate in Mice

As shown in Fig. 1a, on the 6th day of administration, there was no significant difference in tumor volume among the groups of mice; with the extension of administration time, tumor volume gradually showed differences. The combined administration group exhibited significantly lower tumor volume than the model group ($p < 0.01$) and significantly lower than the 5-FU group ($p < 0.01$), as illustrated in Fig. 1b. As shown in Fig. 1c, compared to the model group, both the 5-FU and combined administration groups showed a significant reduction in tumor weight ($p < 0.01$); moreover, compared to the 5-FU group, the combined administration group exhibited a significant decrease in tumor weight ($p < 0.01$). The tumor inhibition rates for the CII-3 group, 5-FU group and combined administration group were 26.24, 49.33 and 74.47%, respectively. The excised tumors were depicted in Fig. 2, it was observed that after 14 days, there was a large difference in tumour size between the groups of mice, with the 5-FU+CII-3 group having the smallest tumour size compared to the model group.

3.2 Influence of CII-3 on Spleen Index and Thymus Index in Mice

As shown in Fig. 3, compared to the normal group, all groups exhibited a significant increase in spleen index (Fig. 3a, $p < 0.01$), the 5-FU group exhibited a significant decrease in thymus index. (Fig. 3b, $p < 0.05$). In comparison to the model group, both the spleen index and thymus index in the 5-FU group showed a significant decrease ($p < 0.01$). When compared to the 5-FU group, the 5-FU+CII-3 group exhibited a significant increase in spleen index and thymus index ($p < 0.05$).

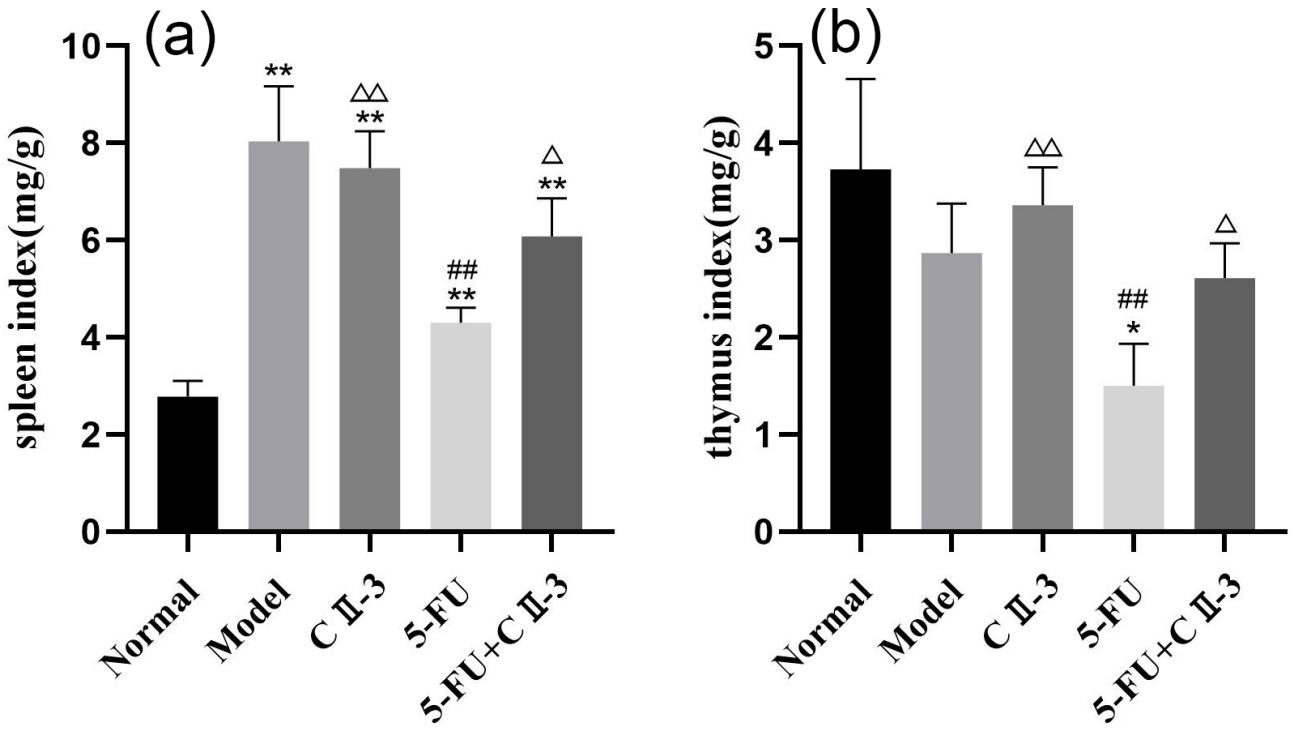

Fig. 3. Changes in organ index under different exposure conditions. (a) Spleen index and (b) Thymus index. n = 3. *$p < 0.05$, **$p < 0.01$: Compared with the normal group, ##$p < 0.01$: Compared with the model group; $\Delta p < 0.05$, $\Delta\Delta p < 0.01$: Compared with the 5-FU group.

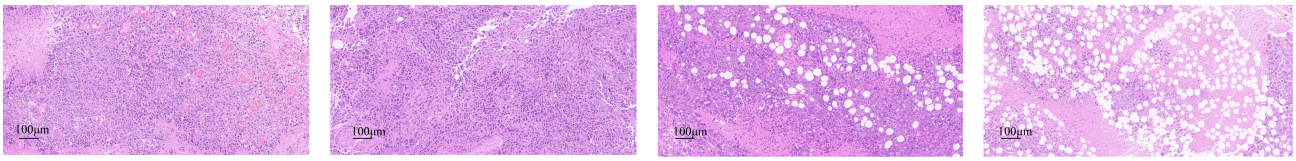

Fig. 4. Changes in histopathological morphology of tumor mass in H22 bearing mice under different exposure conditions (H&E, ×200). (a) Model group, (b) CII-3 group, (c) 5-FU group and (d) 5-FU+CII-3 group. Scale bar = 100 μm. H&E, Hematoxylin and Eosin staining. n = 6.

3.3 Influence of CII-3 on Pathological Morphology of Tumor Tissues in Mice

As shown in Fig. 4a, H&E staining results revealed that the tumor tissues in the model group were characterized by abundant blood vessels, well-preserved cell status with diffuse distribution, no necrotic cells and varying degrees of nuclear staining, clear nucleoli and increased mitotic activity. As shown in Fig. 4b, the CII-3 group displayed loosely arranged tumor tissues with reduced blood supply. As shown in Fig. 4c, following 5-FU treatment, tumor tissues showed areas of necrosis and fragmented tumor cells, a significant decrease in cell number, irregular arrangement of tumor cells and nuclear condensation. As shown in Fig. 4d, the combined administration group exhibited extensive tumor tissue necrosis, significant appearance of lipid vacuoles and obvious nuclear fragmentation.

3.4 Impact of CII-3 on NK Cell Cytotoxicity and T/B Lymphocyte Proliferation Capacity in Mouse Spleen

As shown in Fig. 5, compared to the normal group, both NK cell cytotoxicity (Fig. 5a) and T-cell proliferation capacity (Fig. 5b) significantly decreased in the model group ($p < 0.01$), the 5-FU group displayed a significant reduction in NK cell cytotoxicity (Fig. 5a) and T/B cell proliferation capacity (Fig. 5b,c, $p < 0.01$). Conversely, the CII-3 group exhibited a notable increase in NK cell cytotoxicity (Fig. 5a) and T/B cell proliferation capacity compared to the model group (Fig. 5b,c, $p < 0.05$ or $p < 0.01$). Furthermore, the combined administration group demonstrated a substantial increase in NK cell cytotoxicity (Fig. 5a) and T/B cell proliferation capacity (Fig. 5b,c) following the addition of CII-3, compared to the 5-FU group ($p < 0.05$ or $p < 0.01$).

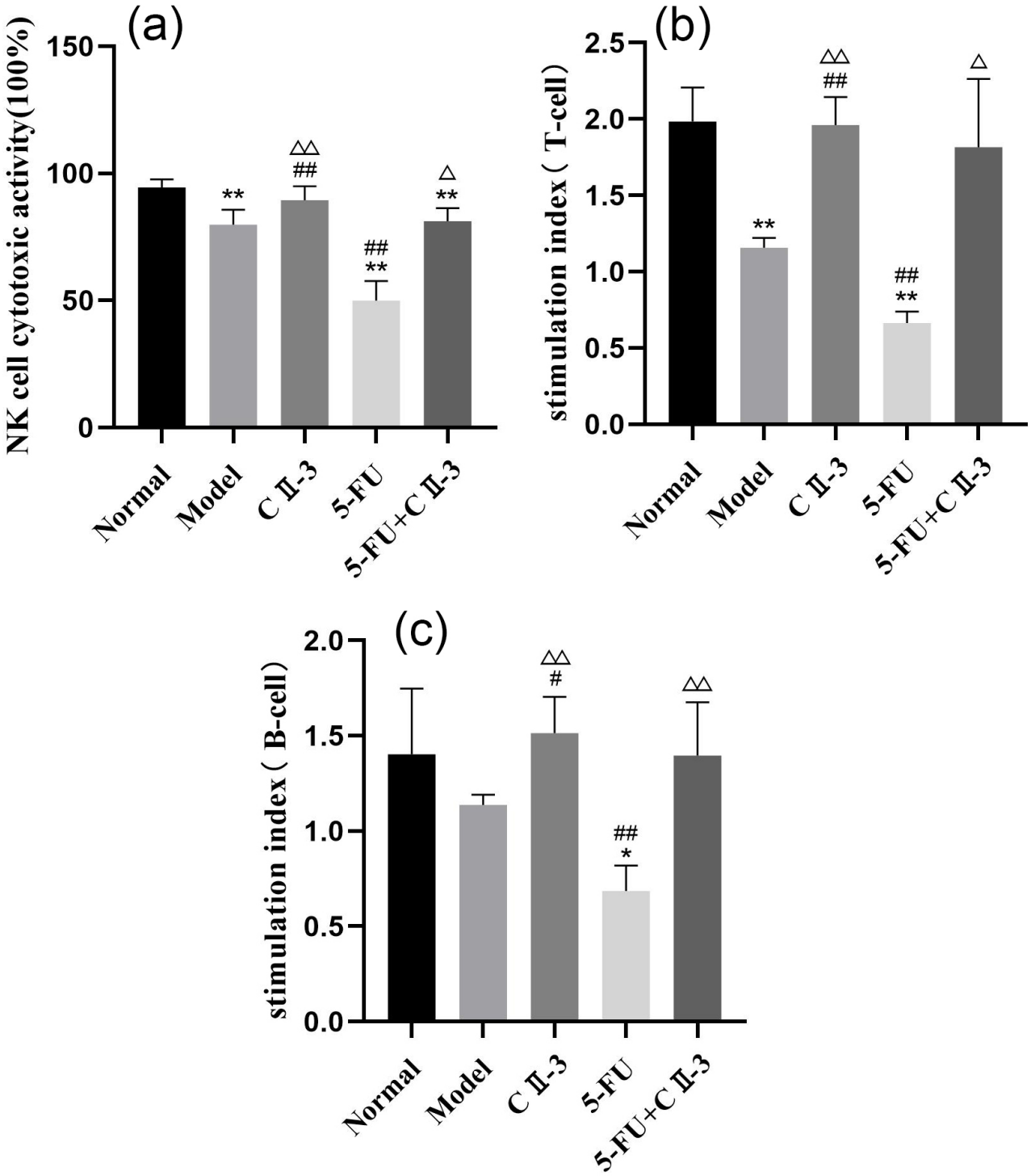

Fig. 5. Changes in immune cells in mice spleen under different exposure conditions. (a) NK cell cytotoxicity, (b) T lymphocyte proliferation capacity and (c) B lymphocyte proliferation capacity. n = 6. *$p < 0.05$, **$p < 0.01$: Compared with the normal group, #$p < 0.05$, ##$p < 0.01$: Compared with the model group; $\Delta p < 0.05$, $\Delta\Delta p < 0.01$: Compared with the 5-FU group. NK, Natural Killer Cells.

3.5 Effect of CII-3 on the Proportion of CD^{3+}, CD^{4+} and CD^{8+} Cells in Mouse Spleen

Fig. 6 shows the results of flow cytometry experiments. As shown in Fig. 7, compared to the normal group, the CD^{3+} (Fig. 7a) and CD^{4+} (Fig. 7b) cell proportions in both the model group and the 5-FU group significantly decreased ($p < 0.05$ or $p < 0.01$). Compared to the model group, the CD^{8+} cell proportion in the 5-

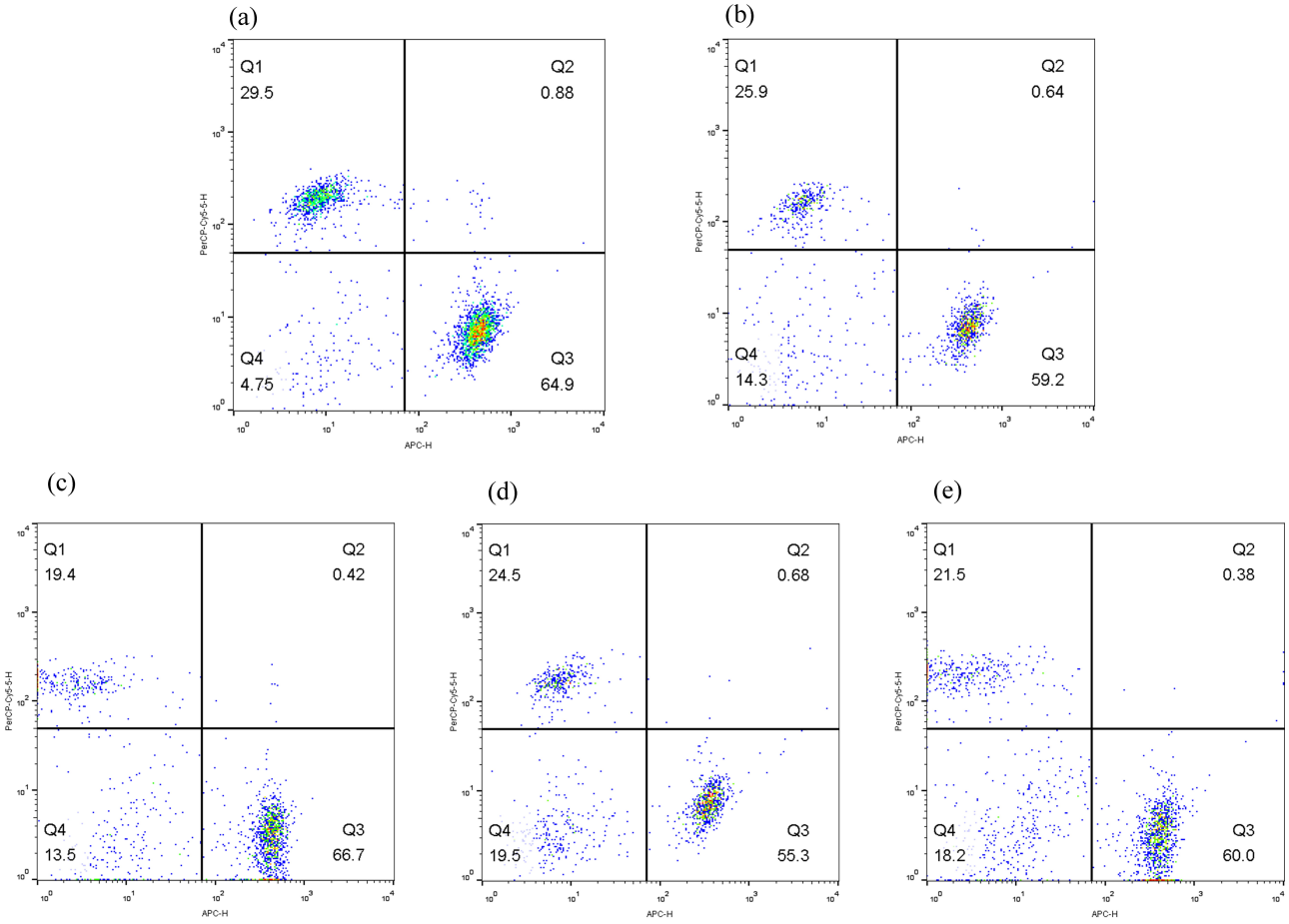

Fig. 6. Flow cytogram of CD3+, CD4+ and CD8+ cells. (a) Normal, (b) Model, (c) CII-3, (d) 5-FU and (e) 5-FU+CII-3. n = 6.

FU+CII-3 group significantly decreased (Fig. 7c, $p < 0.01$) and the CD^{4+}/CD^{8+} ratio significantly increased (Fig. 7d, $p < 0.05$ or $p < 0.01$). Compared to the 5-FU group, the combined administration group showed a significant increase in CD^{3+} (Fig. 7a) proportion, a significant decrease in CD^{8+} (Fig. 7c) proportion and a significant increase in CD^{4+}/CD^{8+} ratio (Fig. 7d, $p < 0.01$).

3.6 Influence of CII-3 on IgA, IgM, IgG and IL-8 Levels in Mouse Serum

As shown in Fig. 8a–c, compared to the model group, the levels of IgA, IgM and IgG in the serum of the 5-FU group mice all decreased ($p < 0.05$). Compared to the 5-FU group, the levels of IgA, IgM and IgG significantly increased after the addition of CII-3 in the combined administration group ($p < 0.05$ or $p < 0.01$). As shown in Fig. 8d, IL-8 in the 5-FU+CII-3 group was significantly lower than that in the model group ($p < 0.05$) and significantly lower than that in the 5-FU alone group ($p < 0.01$).

3.7 Effect of CII-3 on the Expression of TLR4, NF-κB, TRAF6, MYD88 and TNF-α mRNA in Mouse Tumor Tissues

As shown in Fig. 9, compared to the model group, the expression of *TLR4* (Fig. 9a), *MYD88* (Fig. 9d) and *TNF-α* (Fig. 9e) mRNA in the 5-FU+CII-3 group was significantly downregulated ($p < 0.05$ or $p < 0.01$). Compared to the 5-FU group, the combined administration group exhibited a significant downregulation in the expression of *TLR4* (Fig. 9a), *TRAF6* (Fig. 9b), *NF-κB* (Fig. 9c), *MYD88* (Fig. 9d) and *TNF-α* (Fig. 9e) mRNA ($p < 0.05$ or $p < 0.01$).

3.8 Impact of CII-3 on the Expression of TLR4, NF-κB, TRAF6, MYD88 and TNF-α Proteins in Mouse Tumor Tissues

Fig. 10 presented the grayscale images of TLR4, NF-κB, TRAF6, MYD88 and TNF-α proteins in mouse tumor tissues, as shown in Fig. 11. Compared to the model group, the 5-FU group exhibited a significant downregulation in TLR4 protein expression (Fig. 11a, $p < 0.01$) and an increase in TNF-α expression (Fig. 11e, $p < 0.05$). Both the CII-3 group and the 5-FU+CII-3 group showed a significant downregulation in the expression of TLR4, NF-κB and

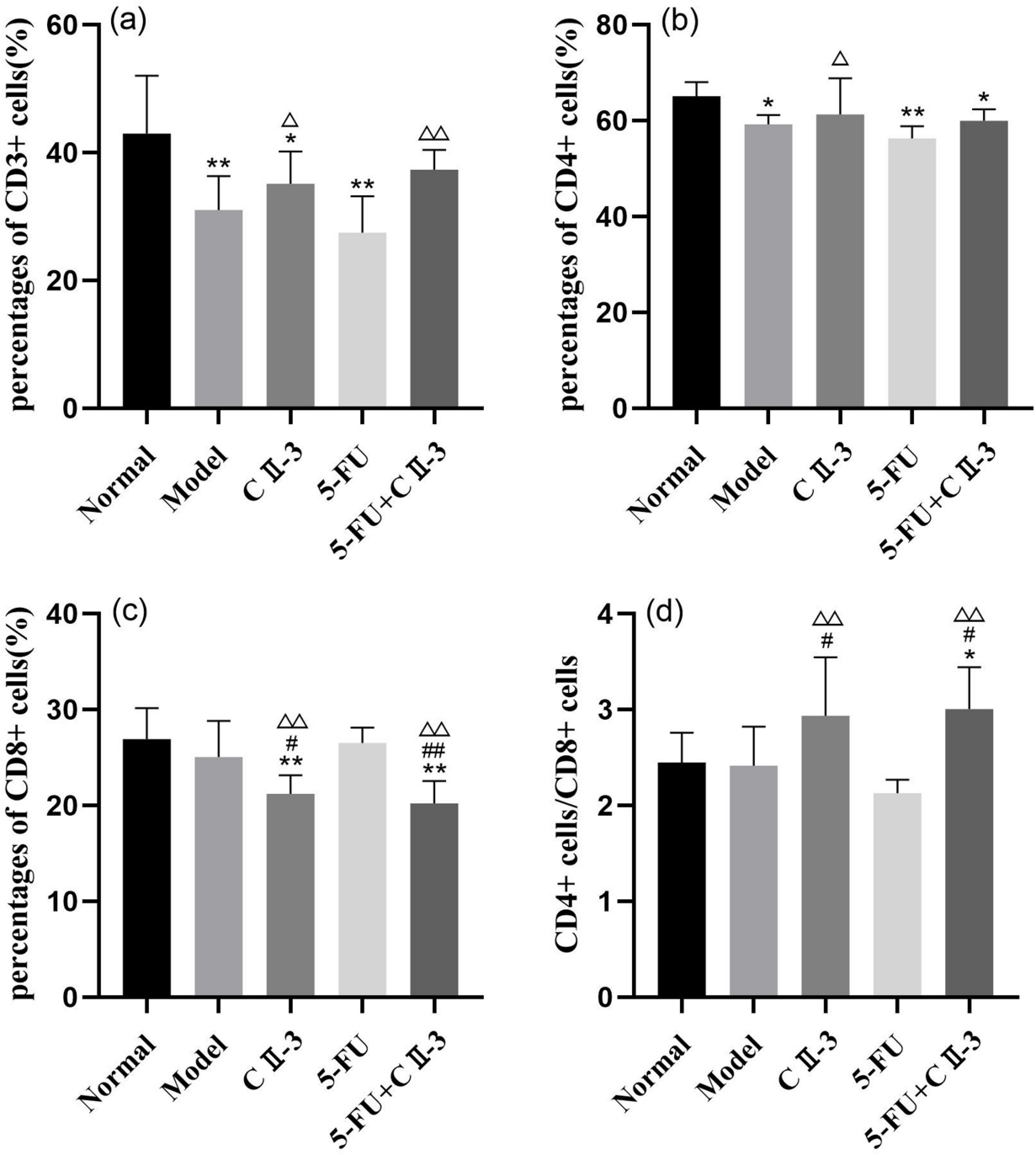

Fig. 7. Changes in the T-cell population in mice spleen under different exposure conditions. (a) CD3+ cells, (b) CD4+ cells, (c) CD8+ cells and (d) CD4+ cells/CD8+ cells. n = 6. *$p < 0.05$, **$p < 0.01$: Compared with the normal group; #$p < 0.05$, ##$p < 0.01$: Compared with the model group; $\Delta p < 0.05$, $\Delta\Delta p < 0.01$: Compared with the 5-FU group.

MYD88 proteins (Fig. 11a,c,d, $p < 0.05$ or $p < 0.01$), with a decrease in TNF-α expression (Fig. 11e) in the 5-FU+CII-3 group ($p < 0.01$). Compared to the 5-FU group, the combined administration group exhibited a significant down-regulation in the expression of TLR4, NF-κB, MYD88 and TNF-α proteins (Fig. 11a,c–e, $p < 0.05$ or $p < 0.01$).

4. Discussion

In the classification of liver cancer based on clinical symptoms in traditional Chinese medicine, it is categorized into patterns such as qi stagnation and blood stasis, liver depression and spleen deficiency, liver-gallbladder damp-heat, liver-kidney yin deficiency, Zheng deficiency blood

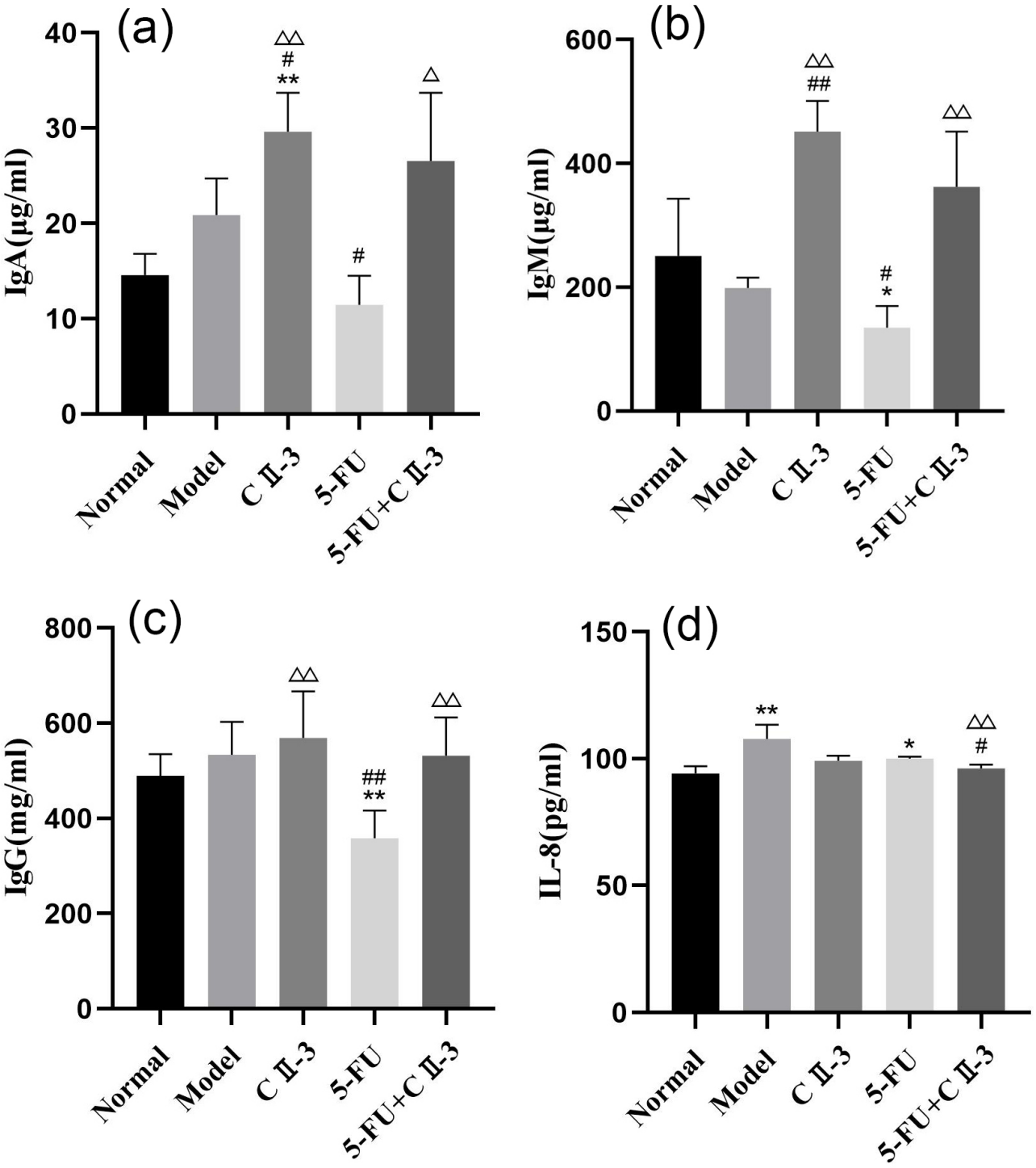

Fig. 8. Changes in the B-cell population and cytokine of mice serum under different exposure conditions. (a) IgA, (b) IgM, (c) IgG and (d) IL-8. n = 6. *$p < 0.05$, **$p < 0.01$: Compared with the normal group; #$p < 0.05$, ##$p < 0.01$: Compared with the model group; $\Delta p < 0.05$, $\Delta\Delta p < 0.01$: Compared with the 5-FU group.

stasis, spleen-kidney yang deficiency and damp-heat toxin accumulation [28]. The *Periplaneta americana*, as documented in the "Shennong Bencao Jing", is described as having effects such as "controlling blood stasis, solidifying lumps, addressing cold and heat, dispersing accumulations, relieving throat obstruction and treating internal cold and infertility" [29]. Acting on the liver meridian, the *Periplaneta americana* is believed to possess functions corresponding to breaking down blood stasis, promoting blood circulation and dispelling stagnation, aligning with the pat-

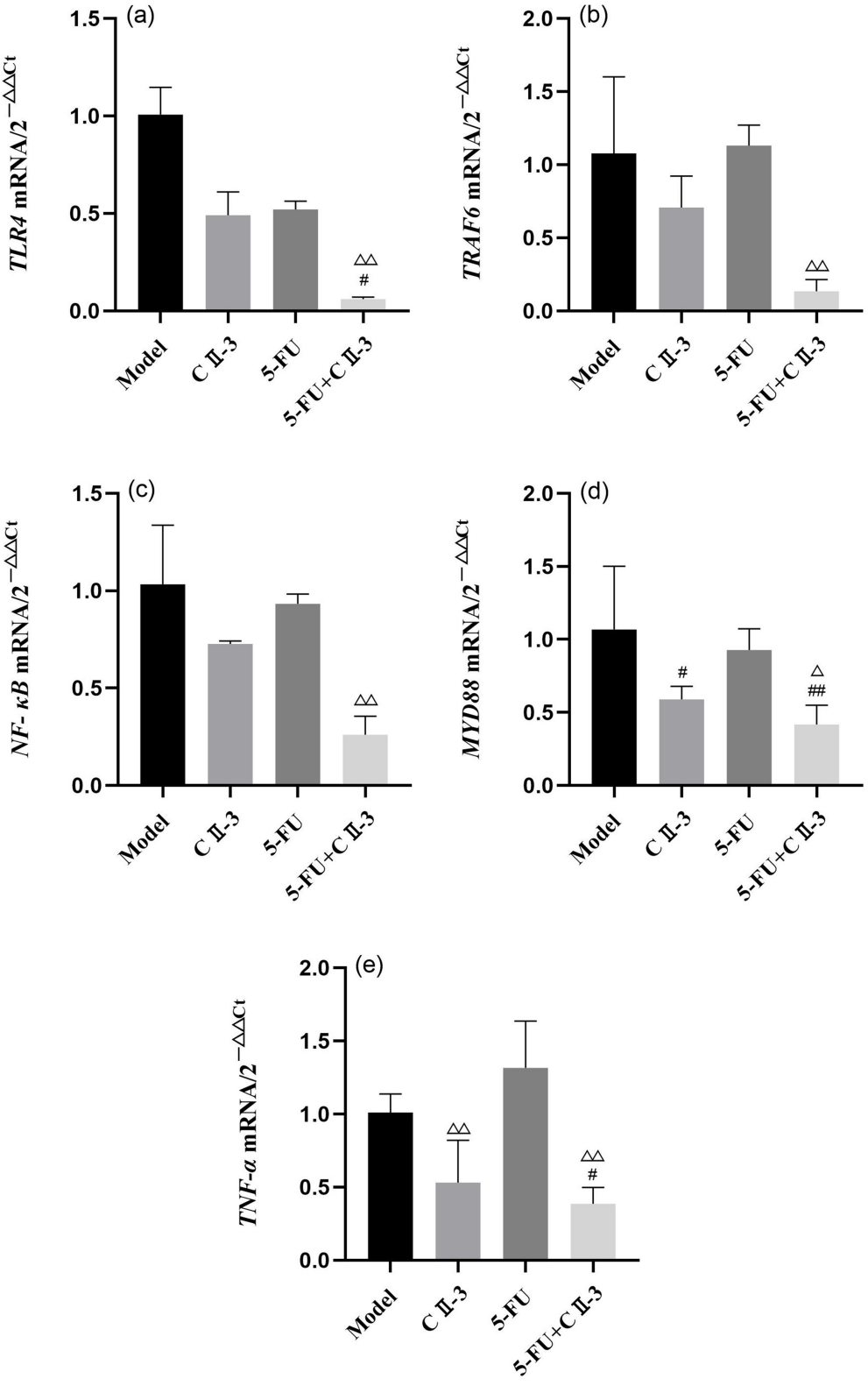

Fig. 9. Changes in expression of, (a) *TLR4*, (b) *TRAF6*, (c) *NF-κB*, (d) *MYD88* and (e) *TNF-α* mRNA in mouse tumor tissues under different exposure conditions. n = 3. #$p < 0.05$, ##$p < 0.01$: Compared with the model group; Δ$p < 0.05$, ΔΔ$p < 0.01$: Compared with the 5-FU group. *TLR4*, Toll-Like Receptor 4; *NF-κB*, Nuclear Factor-kappa B; *TRAF6*, Tumor Necrosis Factor Receptor-Associated Factor 6; *MYD88*, Myeloid Differentiation Primary Response Protein 88; *TNF-α*, Tumor Necrosis Factor-α.

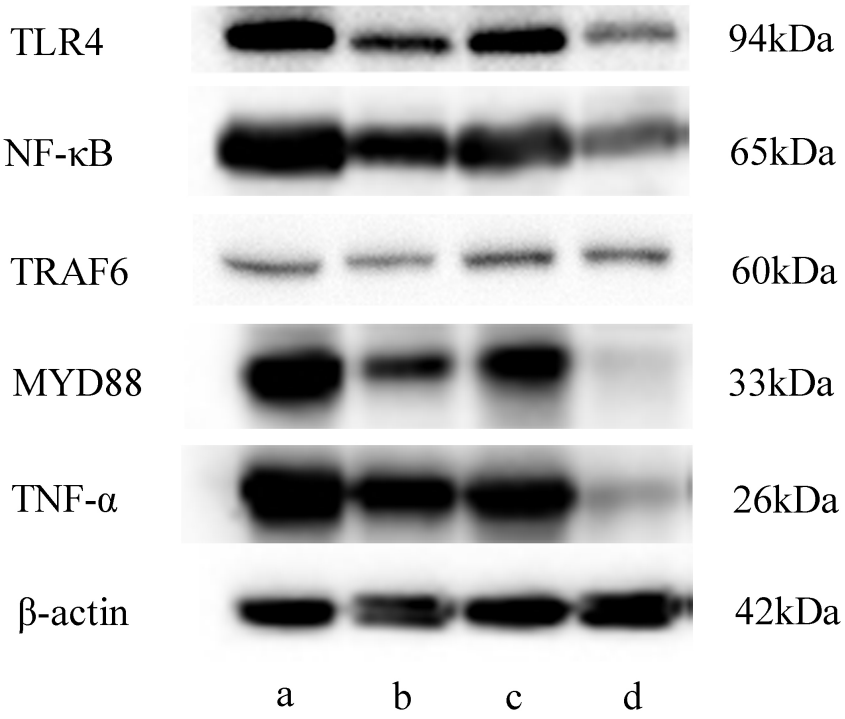

Fig. 10. Gray-scale image obtained using western blot. (a) Model group, (b) CII-3 group, (c) 5-FU group and (d) 5-FU+CII-3 group. n = 3.

terns seen in traditional Chinese medicine for liver cancer [26,30]. Modern medical research indicates significant potential of the *Periplaneta americana* in the treatment of various cancers, particularly in studies related to liver and lung cancers [23].

The CII-3 may exert a comprehensive inhibitory effect on liver cancer through multiple pathways, including immunomodulation and anti-inflammatory effects. Firstly, inflammation in liver cancer has been identified as a crucial factor, playing diverse roles in cancer initiation and progression [31]. Inflammatory processes involve the release of pro-inflammatory cytokines such as TNF-α, IL-6 and IL-1β, which are closely associated with tumor growth, invasion and angiogenesis [32]. The IL-8, an important inflammatory mediator, is linked to tumor development and progression [33]. A significant reduction in IL-8 levels in the 5-FU combined with CII-3 group was observed. Thus, CII-3 may enhance the efficacy of chemotherapy by inhibiting IL-8 production, regulating inflammatory responses and influencing the tumor microenvironment.

Secondly, under the context of 5-FU treatment for liver cancer, the impact on the host immune system becomes a critical consideration. Current experimental results indicated that the combination of 5-FU and CII-3 has a pronounced regulatory effect on the murine immune system, particularly on immune cells and factors. Elevated levels of IgA, IgM and IgG in the 5-FU combined with CII-3 group suggest a potential role of CII-3 in modulating humoral immunity, enhancing the body's defense against infections. Moreover, significant changes were observed in the quantity and activity of immune cells after 5-FU treatment. The NK cells, crucial for nonspecific immune activity, play a vital role in overall immune function [34]. The activation of immune cells is also part of the inflammation in liver cancer [35]. Current results demonstrate that CII-3 can enhance the cytotoxic activity of NK cells, potentially compensating for the inhibitory effect of 5-FU on NK cell activity. This discovery provides a new mechanistic explanation for the immunomodulatory effects of 5-FU combined with CII-3 treatment. The T lymphocytes, especially CD^{3+}, CD^{4+} and CD^{8+} cells, may decrease after 5-FU treatment, leading to an imbalance in T lymphocyte subgroups. This aligns with previous research results, indicating the direct impact of chemotherapy drugs on T lymphocytes.

Research suggested that the activation of the TLR4 signaling pathway in liver cancer cells can increase the production of immune inhibitory factors, promoting tumor cell proliferation and immune escape, leading to the growth and metastasis of liver cancer cells [36,37]. The MyD88-dependent signaling pathway downstream of TLR4 can activate NF-κB, inducing the migration of tumor cells, a phenomenon verified in various cancers [38]. Inhibiting NF-κB can suppress the growth and migration of cancer cells while enhancing their sensitivity to chemotherapy drugs [39]. The TRAF6, as a key factor in the NF-κB pathway, also serves as a regulatory factor for adaptive and innate immunity [40,41]. The TNF-α, regulated by the TLR4/NF-κB pathway, can, under certain conditions, alter the tumor

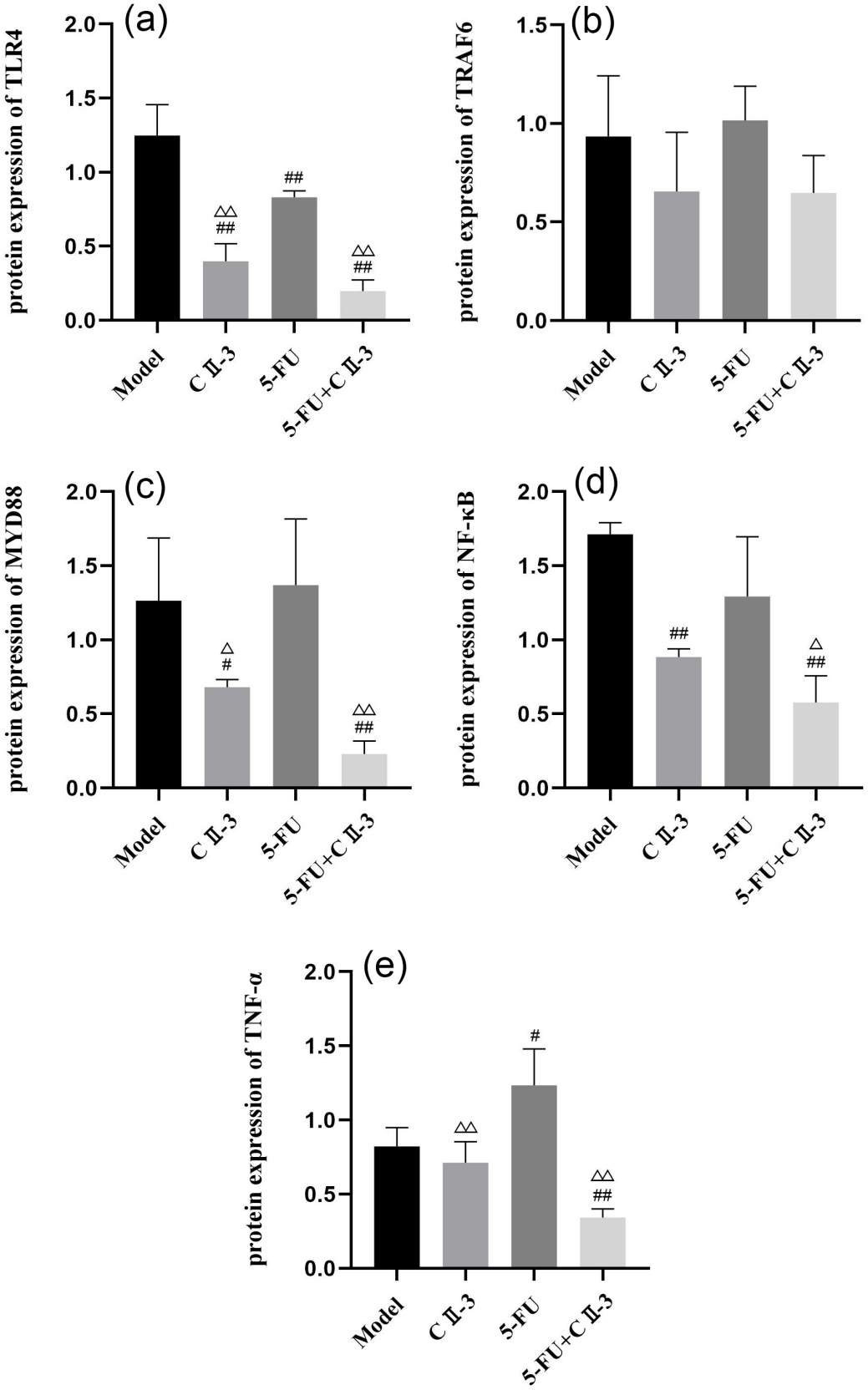

Fig. 11. Changes in expression of, (a) TLR4, (b) TRAF6, (c) MYD88, (d) NF-κB and (e) TNF-α proteins in mouse tumor tissues under different exposure conditions. n = 3. #$p < 0.05$, ##$p < 0.01$: Compared with the model group; $\Delta p < 0.05$, $\Delta\Delta p < 0.01$: Compared with the 5-FU group.

microenvironment, promoting tumor growth, proliferation, invasion, metastasis and tumor angiogenesis [42]. Overexpression of TNF-α may lead to poor prognosis in liver cancer patients [43]. Research results indicated that the mice in the 5-FU combined with CII-3 group exhibited significantly smaller tumor mass and volume than those in the 5-FU group alone, suggesting a tumor-inhibitory effect of the combination. The mRNA and protein levels of TLR4, NF-κB, TRAF6, MYD88 and TNF-α in the 5-FU combined with CII-3 group were significantly downregulated, indicating that CII-3 may enhance the efficacy of chemotherapy by inhibiting the TLR4/MyD88/NF-κB signaling pathway, thereby exerting an inhibitory effect on liver cancer.

This study revealed that 5-FU combined with CII-3 can modulate immune factors and immune cells, improving the immune function of tumor-bearing mice and alleviating the immune suppression state. The 5-FU combined with CII-3 can effectively inhibit the growth of liver cancer and the mechanism may involve the inhibition of the TLR4/MyD88/NF-κB signaling pathway to exert antitumor effects. Further research will delve into the mechanisms of CII-3 in inhibiting tumor growth and modulating immunity, providing experimental and theoretical foundations for the development and application of CII-3 derived from the *Periplaneta americana*. However, it is essential to note some limitations in our study. The experiments primarily focused on murine models and the biological characteristics of mice differ from those of humans. Therefore, caution should be exercised in interpreting the results when applying them to human subjects. Additionally, although we observed the regulatory effect of CII-3 on IL-8, further in-depth research is needed to elucidate the specific molecular mechanisms and signaling pathways involved.

In summary, this research outcomes unveil the multifaceted actions of CII-3 in the treatment of liver cancer, encompassing immunomodulation, anti-inflammatory effects and tumor inhibition. This provides a theoretical foundation for the clinical application of CII-3, but further investigations are warranted to comprehensively understand its mechanisms of action and its potential prospects in clinical therapy.

5. Conclusion

The combination of *Periplaneta americana* extract CII-3 with 5-Fluorouracil (5-FU) demonstrates synergistic anti-tumor and immunomodulatory effects in H22 liver cancer-bearing mice. The CII-3, a complex mixture comprising 25 identified compounds, enhances the inhibitory efficacy on tumor growth, as evidenced by reduced tumor mass and volume. Additionally, CII-3 exerts anti-inflammatory effects by significantly lowering IL-8 levels. These findings provide insights into the potential of CII-3 as an adjunctive therapeutic agent for liver cancer, complementing the effects of conventional chemotherapy. However, caution should be exercised in generalizing these results to human subjects due to species-specific variations. Further research is necessary to unravel the intricate molecular mechanisms underlying CII-3's actions and to explore its clinical applications.

6. Significance Statement

Hepatocellular Carcinoma (HCC) presents a significant threat to human health and life. While chemotherapy stands as a cornerstone treatment for advanced-stage HCC, its efficacy is often hindered by adverse reactions such as immunosuppression. This study aims to identify therapeutic approaches that can enhance chemotherapy effectiveness while mitigating adverse effects. Our research highlights the synergistic anti-tumor and immunomodulatory effects of combined CII-3 and 5-FU treatment, potentially mediated through the regulation of the TLR4/NF-κB signaling pathway. These findings suggest a promising adjunctive role for CII-3 in liver cancer treatment, offering a novel therapeutic strategy.

Availability of Data and Materials

The datasets used and analyzed during the current study are available from the corresponding author on reasonable request.

Author Contributions

RG and GW designed the research study. RY, GW, MG, and XL performed the experiments and curated the data. MG and XL provided guidance on experimental procedures. YW, RG and RY conducted the formal analysis and data visualization. RG and GW developed the methodology. MG acquired the funding. RG, RY, and YW drafted the original manuscript. MG, XL, and YW searched references. MG and XL reviewed and edited the manuscript. All authors contributed to editorial changes in the manuscript. All authors read and approved the final manuscript. All authors have participated sufficiently in the work and agreed to be accountable for all aspects of the work.

Ethics Approval and Consent to Participate

All the experiments were performed based on the approved animal protocols and guidelines established by the Medicine Ethics Review Committee for Animal Experiments of Dali University under the approval (number: 2023P2260).

Acknowledgment

Not applicable.

Funding

This work was supported by the Special Basic Cooperative Research Programs of Yunnan Provincial Undergraduate Universities' Association (202101BA070001-119), the Special Basic Cooperative Research Programs

of Yunnan Provincial Undergraduate Universities' Association (202101BA070001-121), the Open project of Yunnan Provincial Key Laboratory of Insect Biomedicine Research and Development (AT2024002) and the Team Project of Yunnan Revitalization Talent Support Program (No.202305AS350001).

Conflict of Interest

The authors declare no conflict of interest.

References

[1] Shi L, Feng Y, Lin H, Ma R, Cai X. Role of estrogen in hepatocellular carcinoma: is inflammation the key? Journal of Translational Medicine. 2014; 12: 93. https://doi.org/10.1186/1479-5876-12-93.

[2] Li Y, Li H, Spitsbergen JM, Gong Z. Males develop faster and more severe hepatocellular carcinoma than females in kras^{V12} transgenic zebrafish. Scientific Reports. 2017; 7: 41280. https://doi.org/10.1038/srep41280.

[3] Zhang J, Zhang Q, Lou Y, Fu Q, Chen Q, Wei T, *et al*. Hypoxia-inducible factor-1α/interleukin-1β signaling enhances hepatoma epithelial-mesenchymal transition through macrophages in a hypoxic-inflammatory microenvironment. Hepatology (Baltimore, Md.). 2018; 67: 1872–1889. https://doi.org/10.1002/hep.29681.

[4] Zhang ZF, Luo YJ, Lu Q, Dai SX, Sha WH. Conversion therapy and suitable timing for subsequent salvage surgery for initially unresectable hepatocellular carcinoma: What is new? World Journal of Clinical Cases. 2018; 6: 259–273. https://doi.org/10.12998/wjcc.v6.i9.259.

[5] Kim E, Viatour P. Hepatocellular carcinoma: old friends and new tricks. Experimental & Molecular Medicine. 2020; 52: 1898–1907. https://doi.org/10.1038/s12276-020-00527-1.

[6] Hsieh YC, Frink M, Thobe BM, Hsu JT, Choudhry MA, Schwacha MG, *et al*. 17Beta-estradiol downregulates Kupffer cell TLR4-dependent p38 MAPK pathway and normalizes inflammatory cytokine production following trauma-hemorrhage. Molecular Immunology. 2007; 44: 2165–2172. https://doi.org/10.1016/j.molimm.2006.11.019.

[7] Zou H, Wang WK, Liu YL, Braddock M, Zheng MH, Huang DS. Toll-like receptors in hepatocellular carcinoma: potential novel targets for pharmacological intervention. Expert Opinion on Therapeutic Targets. 2016; 20: 1127–1135. https://doi.org/10.1517/14728222.2016.1168809.

[8] Agundez JA, Blanca M, Cornejo-Garcia JA, Garcia-Martin E. Pharmacogenomics of cyclooxygenases. Pharmacogenomics. 2015; 16: 501–22. https://doi.org/10.2217/pgs.15.6.

[9] Yokoyama T, Komori A, Nakamura M, Takii Y, Kamihira T, Shimoda S, *et al*. Human intrahepatic biliary epithelial cells function in innate immunity by producing IL-6 and IL-8 via the TLR4-NF-kappaB and -MAPK signaling pathways. Liver International: Official Journal of the International Association for the Study of the Liver. 2006; 26: 467–476. https://doi.org/10.1111/j.1478-3231.2006.01254.x.

[10] Corrales L, Matson V, Flood B, Spranger S, Gajewski TF. Innate immune signaling and regulation in cancer immunotherapy. Cell Research. 2017; 27: 96–108. https://doi.org/10.1038/cr.2016.149.

[11] Fang H, Ang B, Xu X, Huang X, Wu Y, Sun Y, *et al*. TLR4 is essential for dendritic cell activation and anti-tumor T-cell response enhancement by DAMPs released from chemically stressed cancer cells. Cellular & Molecular Immunology. 2014; 11: 150–159. https://doi.org/10.1038/cmi.2013.59.

[12] Clark SR, Ma AC, Tavener SA, McDonald B, Goodarzi Z, Kelly MM, *et al*. Platelet TLR4 activates neutrophil extracellular traps to ensnare bacteria in septic blood. Nature Medicine. 2007; 13: 463–469. https://doi.org/10.1038/nm1565.

[13] Shi YJ, Gong HF, Zhao QQ, Liu XS, Liu C, Wang H. Critical role of toll-like receptor 4 (TLR4) in dextran sulfate sodium (DSS)-Induced intestinal injury and repair. Toxicology Letters. 2019; 315: 23–30. https://doi.org/10.1016/j.toxlet.2019.08.012.

[14] Yin H, Pu N, Chen Q, Zhang J, Zhao G, Xu X, *et al*. Gut-derived lipopolysaccharide remodels tumoral microenvironment and synergizes with PD-L1 checkpoint blockade via TLR4/MyD88/AKT/NF-κB pathway in pancreatic cancer. Cell Death & Disease. 2021; 12: 1033. https://doi.org/10.1038/s41419-021-04293-4.

[15] Ning Q, Liu YF, Ye PJ, Gao P, Li ZP, Tang SY, *et al*. Delivery of Liver-Specific miRNA-122 Using a Targeted Macromolecular Prodrug toward Synergistic Therapy for Hepatocellular Carcinoma. ACS Applied Materials & Interfaces. 2019; 11: 10578–10588. https://doi.org/10.1021/acsami.9b00634.

[16] Zorzi D, Laurent A, Pawlik TM, Lauwers GY, Vauthey JN, Abdalla EK. Chemotherapy-associated hepatotoxicity and surgery for colorectal liver metastases. The British Journal of Surgery. 2007; 94: 274–286. https://doi.org/10.1002/bjs.5719.

[17] Singh V, Brecik M, Mukherjee R, Evans JC, Svetlíková Z, Blaško J, *et al*. The complex mechanism of antimycobacterial action of 5-fluorouracil. Chemistry & Biology. 2015; 22: 63–75. https://doi.org/10.1016/j.chembiol.2014.11.006.

[18] Arafah A, Rehman MU, Ahmad A, AlKharfy KM, Alqahtani S, Jan BL, *et al*. Myricetin (3,3',4',5,5',7-Hexahydroxyflavone) Prevents 5-Fluorouracil-Induced Cardiotoxicity. ACS Omega. 2022; 7: 4514–4524. https://doi.org/10.1021/acsomega.1c06475.

[19] Zeng D, Wang Y, Chen Y, Li D, Li G, Xiao H, *et al*. Angelica Polysaccharide Antagonizes 5-FU-Induced Oxidative Stress Injury to Reduce Apoptosis in the Liver Through Nrf2 Pathway. Frontiers in Oncology. 2021; 11: 720620. https://doi.org/10.3389/fonc.2021.720620.

[20] Yu YX, Wang S, Liu ZN, Zhang X, Hu ZX, Dong HJ, *et al*. Traditional Chinese medicine in the era of immune checkpoint inhibitor: theory, development, and future directions. Chinese Medicine. 2023; 18: 59. https://doi:10.1186/s13020-023-00751-7.

[21] Huang C, Chen T, Zhu D, Huang Q. Enhanced Tumor Targeting and Radiotherapy by Quercetin Loaded Biomimetic Nanoparticles. Frontiers in Chemistry. 2020; 8: 225. https://doi.org/10.3389/fchem.2020.00225.

[22] Zhang X, Qiu H, Li C, Cai P, Qi F. The positive role of traditional Chinese medicine as an adjunctive therapy for cancer. Bioscience Trends. 2021; 15: 283–298. https://doi.org/10.5582/bst.2021.01318.

[23] Hassan HM, Al-Wahaibi LH, Shehatou GS, El-Emam AA. Adamantane-linked isothiourea derivatives suppress the growth of experimental hepatocellular carcinoma *via* inhibition of TLR4-MyD88-NF-κB signaling. American Journal of Cancer Research. 2021; 11: 350–369.

[24] Ding YF, Peng ZX, Ding L, Peng YR. Baishouwu Extract Suppresses the Development of Hepatocellular Carcinoma via TLR4/MyD88/NF-κB Pathway. Frontiers in Pharmacology. 2019; 10: 389. https://doi.org/10.3389/fphar.2019.00389.

[25] Zhang Y, Lou Y, Wang J, Yu C, Shen W. Research Status and Molecular Mechanism of the Traditional Chinese Medicine and Antitumor Therapy Combined Strategy Based on Tumor Microenvironment. Frontiers in Immunology. 2021; 11: 609705. https://doi.org/10.3389/fimmu.2020.609705.

[26] Wang Y, Zhang Q, Chen Y, Liang CL, Liu H, Qiu F, *et al*. Antitumor effects of immunity-enhancing traditional Chinese medicine. Biomedicine & Pharmacotherapy = Biomedecine &

Pharmacotherapie. 2020; 121: 109570. https://doi.org/10.1016/j.biopha.2019.109570.

[27] Jewett A, Kos J, Fong Y, Ko MW, Safaei T, Perišić Nanut M, *et al*. NK cells shape pancreatic and oral tumor microenvironments; role in inhibition of tumor growth and metastasis. Seminars in Cancer Biology. 2018; 53: 178–188. https://doi.org/10.1016/j.semcancer.2018.08.001.

[28] Zeng C, Liao Q, Hu Y, Shen Y, Geng F, Chen L. The Role of Periplaneta americana (Blattodea: Blattidae) in Modern Versus Traditional Chinese Medicine. Journal of Medical Entomology. 2019; 56: 1522–1526. https://doi.org/10.1093/jme/tjz081.

[29] Xu J, Che Y, Liu X, Liu C, Meng D, Pang X, *et al*. The Regulating Effect of CII-3 and Its Active Components from *Periplaneta americana* on M1/M2 Macrophage Polarization. Molecules (Basel, Switzerland). 2022; 27: 4416. https://doi.org/10.3390/molecules27144416.

[30] Wang Y, Wu Y, Zhou J, Wang Y. Identification of peptides of Periplaneta americana L. extract CII-3 by nano LC-MS/MS. Latin American Journal of Pharmacy. 2023; 42: 1904–1911.

[31] Yuan R, Liu G, Guo M, Liu X. Synergistic and toxicity-reducing effects of Periplaneta americana extract CII-3 combined with CTX on H22 tumor bearing mice. Indian Journal of Pharmaceutical Education and Research. 2023; 57: 1119–1131.

[32] He SY, Zhang CG, Liu H, Zhou Y, Tang ZY, Bi ZY, *et al*. Periplaneta americana extract CII-3 regulates the SIRT1/mTOR signaling pathway and induces senescence of leukemia K562 cells). China Journal of Chinese Materia Medica. 2023; 48: 3039–3045. (In Chinese)

[33] Li ZQ. Traditional Chinese medicine for primary liver cancer. World Journal of Gastroenterology. 1998; 4: 360–364. https://doi.org/10.3748/wjg.v4.i4.360.

[34] Zhao Z, Guo P, Brand E. A concise classification of *bencao* (*materia medica*). Chinese Medicine. 2018; 13: 18. https://doi.org/10.1186/s13020-018-0176-y.

[35] Zou Y, Zhang M, Zeng D, Ruan Y, Shen L, Mu Z, *et al*. *Periplaneta americana* Extracts Accelerate Liver Regeneration *via* a Complex Network of Pathways. Frontiers in Pharmacology. 2020; 11: 1174. https://doi.org/10.3389/fphar.2020.01174.

[36] Zulaziz N, Chai SJ, Lim KP. The origins, roles and therapies of cancer associated fibroblast in liver cancer. Frontiers in Oncology. 2023; 13: 1151373. https://doi.org/10.3389/fonc.2023.1151373.

[37] Zidi I, Mestiri S, Bartegi A, Amor NB. TNF-αlpha and its inhibitors in cancer. Medical Oncology (Northwood, London, England). 2010; 27: 185–198. https://doi.org/10.1007/s12032-009-9190-3.

[38] Cai X, Tacke F, Guillot A, Liu H. Cholangiokines: undervalued modulators in the hepatic microenvironment. Frontiers in Immunology. 2023; 14: 1192840. https://doi.org/10.3389/fimmu.2023.1192840.

[39] Zitti B, Bryceson YT. Natural killer cells in inflammation and autoimmunity. Cytokine & Growth Factor Reviews. 2018; 42: 37–46. https://doi.org/10.1016/j.cytogfr.2018.08.001.

[40] Zhang DY, Friedman SL. Fibrosis-dependent mechanisms of hepatocarcinogenesis. Hepatology (Baltimore, Md.). 2012; 56: 769–775. https://doi.org/10.1002/hep.25670.

[41] Senousy SR, Ahmed ASF, Abdelhafeez DA, Khalifa MMA, Abourehab MAS, El-Daly M. Alpha-Chymotrypsin Protects Against Acute Lung, Kidney, and Liver Injuries and Increases Survival in CLP-Induced Sepsis in Rats Through Inhibition of TLR4/NF-κB Pathway. Drug Design, Development and Therapy. 2022; 16: 3023–3039. https://doi.org/10.2147/DDDT.S370460.

[42] Shi G, Wang C, Zhang P, Ji L, Xu S, Tan X, *et al*. Donor Polymorphisms of Toll-like Receptor 4 rs1927914 Associated with the Risk of Hepatocellular Carcinoma Recurrence Following Liver Transplantation. Archives of Medical Research. 2017; 48: 553–560. https://doi.org/10.1016/j.arcmed.2017.11.011.

[43] Li Z, Gao H, Liu Y, Wu H, Li W, Xing Y, *et al*. Genetic variants in the regulation region of TLR4 reduce the gastric cancer susceptibility. Gene. 2021; 767: 145181. https://doi.org/10.1016/j.gene.2020.145181.